Journal of Thermal Analysis, Vol. 53 (1998) 671-683

NON-DIFFERENTIAL CONDUCTION CALORIMETER, A TOOL TO STUDY THE AFTER QUENCH BEHAVIOUR IN SHAPE MEMORY ALLOYS

A. Isalgué, J. L. Pelegrina and V. Torra*

CIRG, DFA, ETSECCPB, UPC C/. Gran Capità s/n, Campus Nord, B-4, E-08034 Barcelona Spain

(Received December 20, 1997)

Abstract

After the development of differential conduction calorimeters realized by E. Calvet around 1946, the standard equipment always used a differential configuration. In home made systems for special purposes, the instrumentation available nowadays suggests that it is possible to use non-differential conduction calorimeters. In order to prove this, a simple and cheap design was constructed and tested. A sensitivity of 700 mV/W near 298 K (in agreement with the detecting semiconductors), a noise around 0.3 μW and a long time fluctuation of the base line lower than 1 μW were obtained. The reliability of the system was evaluated by analyzing the changes of single crystals of Cu–Zn–Al Shape Memory Alloys after different thermal treatments. The calorimeter allowed the determination of a reproducible set of time constants related to the heat treatments and to the mass (or shape) of the sample. It is concluded that the experimental configuration used is suitable for this isothermal analysis.

Keywords: conduction calorimeters, martensitic transformation, quench effects

Introduction

Heat conduction calorimeters were designed to measure the dissipated heat power, either directly or after an appropriate signal processing [1]. Within the linear domain of the system [2], and avoiding uncontrolled heat fluxes or rearrangement effects inside the cell, the integration of the calorimetric curve (response of the system) provides the total dissipated energy. The first conduction calorimeter was constructed by Tian [3]. It was a non-differential system with only one measuring cell surrounded by thermal detectors. In this case the detection device consisted of an iron-constantan thermobattery of 42 thermoelements

* Permanent address: Div. Metales, Centro Atómico, 8400 S.C. de Bariloche, Argentina.

1418–2874/98/ $ 5.00

Akadémiai Kiadó, Budapest
Kluwer Academic Publishers, Dordrecht

and a galvanometer. This calorimetric equipment had a sensitivity of around 15 mV/W. The limit of the resolution of Tian's calorimeter, taking into account the characteristics of the galvanometer, was estimated to be around ±0.1 μW [4]. The corresponding full scale was near 1000 times this resolution, i.e. near 0.1 mW. Then, it was necessary to reduce the sensitivity through a voltage divider (or via Joule or Peltier compensation effects) when measuring large signals. The introduction (around 1946) by Calvet [1, 4, 5] of a twin element with a differential configuration, smoothed the effects of room temperature fluctuations. This equipment permitted measurements that last some days with a resolution near 0.1 μW.

After Calvet's work, only differential systems were constructed, avoiding any analysis about the possible advantages of a non-differential configuration. Since temperature variations affect the system dynamically, it is necessary that the sensitivities and responses (or transference functions) of the two measuring elements are identical at all temperatures. The identity of the two differential elements is technologically difficult to achieve and the use of a different material for the reference sample always implies an intrinsic difference between the sample and the reference cells. The first criticism concerning the efficiency of differential calorimeters can be found in [6] and references therein, and [7].

The greater resolution of the new analogue or digital instruments available for temperature control as well as for measurements (1 to 100 nV with 6 to 9 significant figures), did not induce an increase in performance of the calorimeters. The practical resolution approaches the limit determined by the Johnson noise (usually around 5 nV). Then, it is possible to make a direct connection of the calorimetric sensor to a digital multimeter (DMM) with an adequate resolution. In this way, taking advantage of the available full scale of the DMM, there is no need to use amplifiers which always produce a loss of linearity, nor to reduce the sensitivity of the equipment for higher signals. Also, the new thermostats (avoiding power failure) have a resolution and long term stability close to 0.01 K, suggesting the possibility to operate without a differential element for isothermal measurements.

In many commercial instruments (sensitivity near 100 mV/W) that usually operate between 225 and 800 K, the noise is close to 10 μW, for a sample volume between 0.02 cm^3 and 1.5 cm^3. In systems that operate at constant temperature (sample volume about 10 cm^3), the noise level approaches 0.5 μW. For instance, the noise and the base line drift of a standard isothermal differential calorimeter (Arion Electronique, BCP type) exceeds 1 μV when the stirring device operates [8]. In home made systems, a compromise has to be achieved between the electromagnetic high frequency noise, the low frequency noise associated with the base line drift, the sensitivity, the available full scale and the upper frequency needed for the analysis of calorimetric curves. Nowadays, the evaluation of all these aspects is necessary to optimize the equipment for each type of measurement, contributing to the simplification of the measuring process and the associ-

ated numerical treatment, and to the reduction of the price of the calorimetric device. Recently, in the nanosized calorimetric analyzers [9] non-differential detectors were used and, eventually, cause-and-effect filtering of base line perturbations. The method uses a transfer function established between the external temperature and related baseline. In a world with increased computer availability and larger full scale of DMM, criticism to standard calorimetry increases progressively [7, 10–14]. The suppression of the differential design will reduce experimental complexity in several fields. For instance, in reference [15] this was suggested for gas chromatography.

For the study of Cu–Zn–Al shape memory alloys (SMA), standard equipment provides poor resolution to visualize the details of microprocesses. It was necessary to design specific calorimeters, which allowed the evaluation of the latent heat between the metastable phases with high reliability and good temperature resolution. In particular, the SMA characteristics of the transformation (metastability and burst processes, internal stresses, temperature changes, dislocation creation and hysteresis) required the improvement of the capabilities of conduction calorimeters (see for instance [16] and references therein). The first design used, according to the tendencies of that moment (derived from older isothermal systems developed around 1965 (see for instance [17]), was a differential one, together with spontaneous cooling and heating in order to minimize the temperature control effects (sample volume ≤ 0.5 cm^3, temperature range between 100 to 373 K) [18–20]. The second one introduced temperature control by means of an improved automatic system (Peltier based) for systematic cycling studies [21–24] with filtering of the noise induced by the temperature control on calorimetric curve [22].

The isothermal behaviour of SMA after thermal treatments is a recurrent and unsolved problem. It is related to the diffusion processes which occur and are responsible for the elimination of vacancies and for changes in the degree of B2 and/or $L2_1$ order in the alloy. The analysis of the changes in the transformation temperatures in Cu–Zn–Al alloys [25] and the released energy after quenching [26] has been done with differential systems operating at constant temperature. The main result, related to dynamic phenomena associated with the previous quench, indicates a dissipated heat with an undetermined or varying time constant [26]. This result is difficult to accept when one compares it with resistance measurements as a function of time and temperature [27, 28]. To determine quantitatively the dynamic parameters of the energy dissipation of the SMA (either in the parent or in the martensitic phase), it is necessary to have sufficient sensitivity and stability of the calorimetric device for the measurement of processes that can last several days. This implies again that it is of great importance to avoid the base line drift induced by the fluctuations in ambient temperature.

In this work a low price non-differential calorimetric system was built. The system was used at constant temperature. The experimental analysis furnished a preliminary evaluation of the suitability of non-differential systems in long last-

ing measurements and permitted determination of the dynamic parameters of the energy dissipation produced after quench in Cu–Zn–Al shape memory alloys.

Experimental

A low price calorimetric system, shown in Fig. 1, was designed to operate at constant temperature. The reference temperature was provided by the inner copper block and was measured by means of a Pt-100 resistance, located in a hole of the block. A Melcor FC-0.6-66-06-L thermobattery was used as the calorimetric sensor (available surface about 1 cm^2). The thermal fluctuations of the external bath, which would be transmitted to the reference block, are smoothed by a multiple layer system, consisting of four stainless steel closed cylinders (external diameter 8.9 cm and height 18.2 cm). They were denoted as S_1, S_2, S_3 and S_4 and had a wall thickness of 0.2 cm. The cover of each cylinder can be pulled out to allow mounting of the system. The covers had a central 1 cm diameter hole for the passage of the sample holder and a smaller one on the slide for the electrical wires. Between S_3 and S_4 (as also between S_1 and S_2) three cylindrical plastic separators were put to insure the alignment of the system, and the space between them was filled with alumina wool to provide thermal insulation. S_2 and S_3 were separated by a set of metallic feet and the cavity was filled, except the upper end, with car antifreezing liquid (a solution of ethylene glycol in water) to increase heat capacity and reduce temperature fluctuations. The calorimetric sensor was aligned with the holes of the covers to allow for an easy sample manipulation.

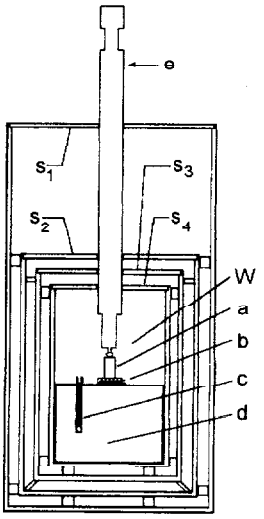

Fig. 1 Calorimetric device. a: sample, b: melcor thermobattery, c: Pt100 resistance, d: copper block, e: sample holder, W: working space, S_1, S_2, S_3 and S_4: metallic layers. The insulation between the layers is not shown (only the separators)

The electrical wires formed a horizontal loop in each cavity between the successive covers before they passed to the following one. The sample holder was made of plexiglass and the sample was attached with a small piece of adhesive ribbon. The calorimetric system was partially (75%) immersed in a Lauda RL6 thermostat. The available depth of the thermostat bath was about 14 cm. The thermostat and the measuring system were placed inside an air-conditioned room.

Three HP3478A digital multimeters were used to acquire the following data: the calorimetric response (100 nV resolution and 30 mV full scale), the temperature by means of a Pt100 resistance (1 mΩ resolution and 300 Ω full scale) and the voltage on a calibrated resistance used for the Joule effect analysis (calibration). The data were stored in a computer (PC-AT 286) through the GPIB bus and the control was performed with a QUICKBASIC program. It was possible to take readings of the calorimetric curve every 0.6 s. The calibration of the system was done at 267.0 K and 298.2 K, and the measurements were performed at 298.2 K.

From a single crystal of a Cu - 16.06 at% Zn - 15.97 at% Al alloy, two samples were cut with masses m_1=0.485 g and m_2=1.304 g. They transformed martensitically at an estimated M_S temperature of 230 K. Therefore, at the working temperature, the samples were in the parent or β phase. The samples were homogenised for 1080 s at 1123 K and then either quenched in water or air cooled (the latter process lasts 300 s) in both cases, additional 30 s were necessary to manipulate the sample. After this the sample was placed for 60 s inside a local bath immersed in the thermostatic bath to ensure a reference temperature. Afterwards, the sample was removed from the bath, dried, fixed to the holder (which was at the internal temperature of the calorimeter) and put inside the calorimeter, this process took less than 60 s. Usually, to have a well defined starting point, the data acquisition for each measurement began 900 s before the introduction of the sample inside the furnace.

Results and discussion

Basic parameters of the non-differential calorimeter

In Fig. 2, the baseline is shown at 298.2 K as a function of time. Taking into account the sensitivity, it was found that the resulting noise was around ±0.2 μW and the combined action of the noise and the baseline drift did not exceed 1.4 μW peak to peak. Also, the fluctuation of the temperature inside the calorimeter was smaller than the resolution of the DMM that has been used (±1 mΩ equivalent to 0.005 K peak to peak).

The calibration was done using Joule dissipation in the stationary state (Heaviside signal). This also served as a preliminary study of the capabilities of the calorimetric system (Fig. 3). For this purpose a constantan resistance was put inside a copper box of the same volume as the SMA samples and different electrical currents were applied. The results are shown in Table 1, together with the resulting sensitivity. The average value of the sensitivity S was (675±3) mV/W at

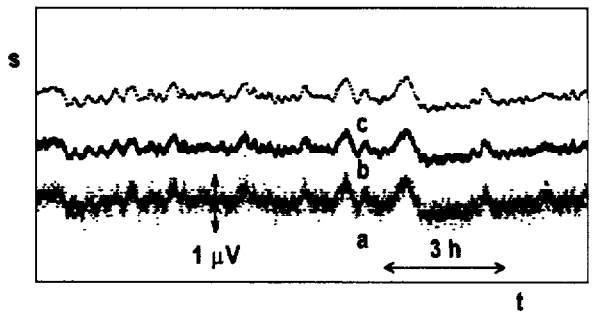

Fig. 2 Stability of the baseline with time showing the action of noise and drift effects: a) baseline, b) filtered baseline (0.1 Hz Shannon cut-off), c) filtered baseline (0.01 Hz Shannon cut-off)

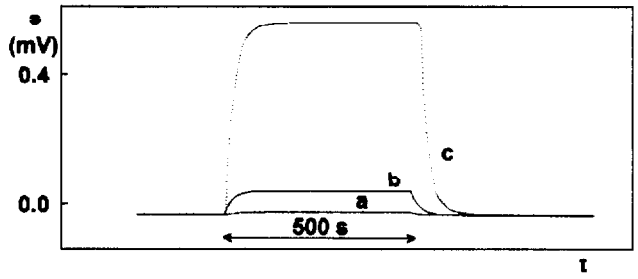

Fig. 3 Calorimetric curves as a function of the time for three dissipated powers for calibration using Joule effect (a, b, c as in Table 1)

298.2 K and (612±2) mV/W at 267.0 K. It was found that in the range of the dissipated powers used, the variation of the sensitivity is lower than 0.3%. From the calorimetric curves associated with the Joule effect, the first time constant τ_0 was evaluated as 19.4±0.9 s, and a negligible temperature dependence was found. The sensitivity and the value of τ_0 are dependent on the thermal properties of each sample (heat capacity, thermal conductivity), on the thermal resistance of the contact between the sample and the calorimetric sensor, and, in the worst case, on the thermal link between the sample and the sample holder. Therefore, it is necessary to work always with samples and calibration devices of the same shape, in order to eliminate the contributions of these perturbations. A complete quantitative analysis of the accuracy of this calorimetric system goes beyond the scope of this work (a preliminary outline of the method appears in [7]).

Sample positioning

The placement of the sample induces a transitory phenomenon that masks the initial part of the calorimetric curves. To evaluate this effect, measurements were taken on the sample without thermal treatment and at the reference temperature

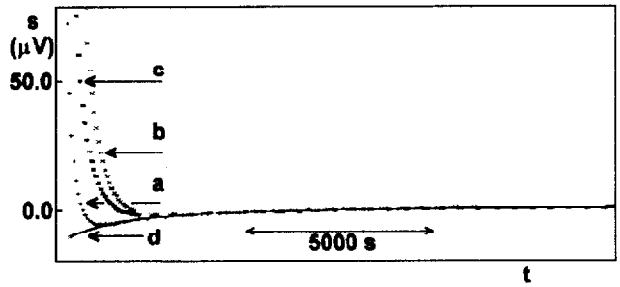

Fig. 4 Calorimetric curves corresponding to the introduction of the same sample (mass m_1) in three ways: a (+), b (x), c (•), d: Fitted lines from the estimated amplitudes and time constants, omitting the stochastic transitory part

Table 1 Sensitivity measurements using Joule effect (a, b and c are related to Fig. 3).

Tl K		*Wl* mW	*s/n*	*N*	*Sl* mV/W
	a	14.1	20	6	617.8
267.0	b	104.3	200	3	611.6
	c	897	1800	3	610.1
	a	14.3	20	3	692.0
298.2	b	103.0	200	6	676.5
	c	902	1800	3	673.6

W: input Joule effect; *s/n*: calorimetric signal-to-noise ratio; *N*: number of measurements; *S*: sensitivity

of the thermostat. In Fig. 4 the reproducibility of different runs is shown. It can be seen that the stochastic initial part of the curves disappears in less than half an hour. Afterwards the same behaviour is followed and two time constants (τ_2 and τ_4 in Table 2) can be deduced for each sample using inverse filtering. In can also be seen that their values are dependent on the mass (or shape) of the sample. From these time constants, the amplitudes a_i were evaluated in order to allow a rough estimation of the induced disturbance on the measured energy due to the introduction of the sample. The random effects associated with this process (including inhomogeneous temperature profiles) can be considered to last about 2000 s. Omitting this initial part of the curve, the numerical fits confirm the reliability and resolution (~1 μW) of the device for isothermal studies of low power, long-time phenomena (see the fitted line in Fig. 4).

Thermal treatment effects

In Fig. 5 the reproducibility of the measurements for each heat treatment can be clearly seen. The air cooled case corresponds to curves A and the water

quenched case to curves B. Curves C represent the positioning of the sample without any heat treatment. In Fig. 5a, the short-time behaviour (t<1200 s) can be seen. The water quenched sample shows a greater dissipation than the air cooled one. For times ~10000 s (Fig. 5b) a change in behaviour between heat treatments can be observed. In this domain, the signal difference between air cooled and water quenched specimens exceeds 4 μW for the larger mass. In Fig. 5c (108000 s full scale), the long-time tail is shown, including the noise and drift. The continuous lines correspond to the fits made using the evaluated time constants (Table 2) and the associated amplitudes. As in the sample positioning analysis, the time constants were obtained by an initial standard filtering and the amplitudes by a trial and error subtraction of the curves. It is to be noted that in the set of time constants, those corresponding to the positioning of the sample are also established. In Table 2 the mass (or shape) dependence of the time constants is clearly seen. In Table 3 a preliminary evaluation of the dissipated energies is given using two time constants for the small mass, and two and three for the larger. It can be seen from these results that it is necessary to take into account all the contributions (the complete set of time constants) for a correct evaluation of the dissipated energy.

Table 2 Time constants τ_i (in 10^3 s) corresponding to the two masses used: m_1 (small) and m_2 (large). PS: values associated with the placement of the sample; AC: air cooled; WQ: water quenched. The values are classified according to the possible origin of the dissipation

Mass		τ_1	τ_2	τ_3	τ_4	τ_5
	PS	–	6	–	1.0	
m_1	AC	30	6	1.5	–	–
	WQ	17	6	2.5	–	–
	PS	–	10	–	1.7	–
m_2	AC	40	10	7.0	1.7	–
	WQ	17	10	4.2	1.7	1.0

The above results show that, after the initial stochastic perturbation related to the sample insertion, a remarkable reproducibility is obtained for the measurements on samples with the same thermal treatment. The time constants associated with sample positioning reappear in each curve, independently of the thermal treatment (Table 2). If, as it seems to be the case, the time constants are greater than those corresponding to the Joule effect (transfer function) and to the sample insertion, their values can be measured and therefore correlated with the intrinsic processes occurring inside the sample (see Appendix). Therefore it seems that this calorimetric design is suitable for providing reasonably good results. A point to be analyzed carefully is the integration back to the exact 'end' of the heat treatment, which obviously needs an explicit definition of the time ori-

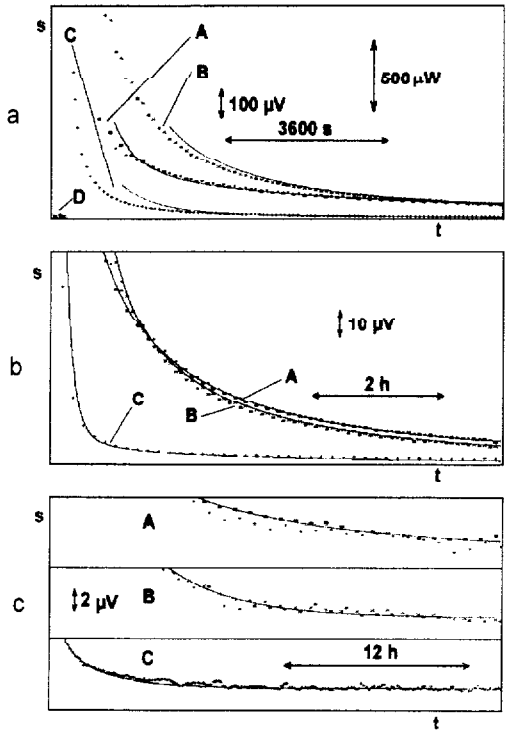

Fig. 5 Reproducibility of the calorimetric curves associated with different thermal treatments for the larger mass. The continuous line is constructed with the fitted time constants. A: air cooled; B: water quenched; C: placement of the sample without heat treatment; D: baseline, before sample positioning. a) initial part of the calorimetric curves; b) difference in behaviour between water quenched and air cooled samples; c) the long time tail allows to evaluate reproducibility, noise and/or drift

gin after each heat treatment. In fact, the time elapsed during the cooling process is dependent on the type of quench and can be masked by the initial transitory. Therefore, the calorimetric response deserves a thorough analysis to recover the parameters of the change of the material. The appearance of different time constants shows a way to analyze the intrinsic phenomena connected with the heat treatments. The mean internal state is a function of the local cooling rates and, as a heat transfer problem, is shape dependent. In this sense, the thickness seems to be the critical length for small samples in the course of a heat treatment, whereas the diameter for large samples. An interpretation (out of the scope of this work), based on the changes in of the atomic order, needs a microscopic model and/or rules to take into account the shape of the sample.

It was shown that, with this device, it is possible to detect several and reproducible time constants by performing several runs in the samples. For that reason, it seems to be inadequate to assign a continuous change to the time constant for the numerical treatment, as performed in [26].

Table 3 Dissipated energy (J g^{-1}) evaluated by subtracting the effect of sample placement for the small (m_1) and large mass (m_2); a) using the first two time constants; b) using three time constants

	Air cooled	Water quenched
m_1 (a)	0.85	0.80
m_2 (a)	0.43	0.38
m_2 (b)	0.95	0.75

Conclusion and perspectives

It was shown that an elementary non-differential calorimeter allows to carry out reliable experiments that can last several days. The measurements taken had a resolution of ±0.7 μW, taking into account noise and baseline drift. The results obtained from two different thermal treatments demonstrated that the system has an appropriate resolution to analyze the changes of Cu–Zn–Al alloys. It was also possible to evaluate different time constants associated with the internal changes of the samples, which depend on the mass (or shape) of the sample and on the nature of thermal treatments. The perturbation produced by the introduction of the sample into the calorimeter could be eliminated because the corresponding time constants could be identified. The mass (or shape) dependence was expected, since it affects the internal temperature distribution due to the different thermal gradients which appear after each kind of treatment. Quantitative results require standardization of the sample shape and mass and working hypothesis about the 'end of the heat treatment'. The equipment showed an adequate precision for the study of the dynamics (time constants) of the process. Due to the intrinsic problem of the definition of the time origin, the energy is expected to be less well established.

The present results indicate that the differential setup in conduction calorimeters is not always necessary. Fifty years after Calvet's work, thanks to the reliable behaviour of thermostats and to the available instruments, the potential advantages of the non-differential systems in long-time measurements can be utilized. These advantages include, for instance, reduced price and volume and, also, a less complex theoretical model for the calorimetric setup with a reduced set of parameters.

A revision of the present standard equipment can be profitable, if accuracy or experimental improvement is the main objective. For instance, a part of the baseline drift in a programmed temperature variation is related with intrinsic differences between reference and measurement crucible. Eventually, a separate analysis of the outputs of the sample and the reference (the differential system is recovered via software) will provide new insight in the calorimetric work. At the

present state of the art, the feedback between the reliability of the results (affected by the uncontrolled heat fluxes and/or rearrangement effects inside the cell), the physical characteristics of the measurements (noise, signal to noise ratio, length in time, protected/unprotected samples from external ambient temperature effects) and the available performance of the equipment (resolution, full scale, sampling) seem to be of decisive role in the appropriate choice of equipment for improved and accurate thermodynamic and kinetic measurements.

Appendix

Exponential heat dissipation and long-time behaviour

Using an RC model, the form of the transference function TF in Laplace (p) or time (t) representation associated to a dissipation realized in only one volume element, can be written as

$$TF(p) = S\frac{\prod_{j=1}^{M}(\tau_j^* p + 1)}{\prod_{i=1}^{N}(\tau_i p + 1)} = \sum_{j=1}^{N}\frac{a_i}{p + \omega_i}$$

$$TF(t) = \sum_{i=1}^{N} a_i e^{-t/\tau_i} = \sum_{i=1}^{N} a_i e^{-\omega_i t}; \qquad S = \sum_{i=1}^{N} a_i \tau_i$$

S being the sensitivity, τ_j^* relate the zeros, τ_i the poles, N and M integers, a_i coefficients and $\omega_i = 1/\tau_i$.
If the dissipated heat $W(t)$ has one or more exponential terms, it can be written as

$$W(t) = \sum_{k=1}^{L} a_k^w e^{-t/\tau_k^w} = \sum_{k=1}^{L} a_k^w e^{-\omega_k^w t}$$

Then, the calorimetric curve s in Laplace or time representation results

$$s(p) = TF(p)W(p)$$

$$s(t) = \int_0^t TF(t^*)W(t - t^*)\mathrm{d}t^* = \int_0^t \left(\sum_{i=1}^{N} a_i e^{-\omega_i t^*}\right)\left(\sum_{k=1}^{L} a_k^w e^{-\omega_k^w (t-t^*)}\right)\mathrm{d}t$$

$$= \sum_{i=1}^{N} a_i \left(\sum_{k=1}^{L} a_k^w e^{-\omega_k^w t} \int_0^t e^{-\omega_i t^*} e^{\omega_k^w t^*} dt^* \right)$$

$$= \sum_{i=1}^{N} a_i \left(\sum_{k=1}^{L} a_k^w \frac{1}{\omega_k^w - \omega_i} \left[e^{-\omega_k^w t} - e^{-\omega_i t} \right] \right) \equiv \sum_{i=1}^{N} b_i e^{-\omega_i t} + \sum_{k=1}^{L} c_k e^{-\omega_k^w t}$$

It can be seen that the curve includes all exponential terms. The series of time independent coefficients b_i and c_k includes the contributions of the transference function as also of the dissipated heat.

At the long time tail, using a as a working hypothesis that

$$\omega_k^w << \omega_i \quad \forall k,i \quad \text{and} \quad t > \tau_i \quad \forall i$$

the behaviour of the curve reduces to

$$s(t > \tau_i) \approx \left(\sum_{i=1}^{N} a_i \tau_i \right) \left(\sum_{k=1}^{L} a_k^w e^{-\omega_k^w t} \right) = SW(t)$$

Therefore, the calorimetric curve is proportional to the heat power supplied by the sample, allowing to recover its parameters in an easy way.

* * *

Research carried out under the project NATO 920452 (Calorimetric instrumentation development). The CICYT and EEC ALA/MED projects are acknowledged for partial support. J. L. Pelegrina thanks DGU (Generalitat de Catalunya) and CONICET for financial support. Fruitful discussions with Prof. H. Tachoire (LPCM - Thermochimie, Univ. Provence, France), Dr. F.C. Lovey and Dr. A.J. Tolley (CAB-Argentina) are gratefully acknowledged.

References

1 E. Calvet and R. Pratt, 'Microcalorimetrie', Masson, Paris, 1956 (in French).
2 E. Rojas, V. Torra and J. Navarro, An. Fis., 67 (1971) 359 (in Spanish).
3 A. Tian, 'Recherches sur la calorimétrie par compensation – Emploi des effets Peltier et Joule – Étude d'un microcalorimètre intégrateur, oscillographe et ballistique', Louis Jean Ed., Gap 1933 (in French).
4 E. Calvet, Mémoriel des Services Chimiques de l'État, 32 (1946) 162 (in French).
5 E. Calvet, C. R. Acad. Sci., 226 (1948) 1702 (in French).
6 M. Rodriguez de Rivera, H. Tachoire and V. Torra, J. Thermal Anal., 41 (1994) 1385; H. Tachoire and V. Torra, Thermochim. Acta, 266 (1995) 239.
7 V. Torra and H. Tachoire, J. Thermal Anal. Cal., 52 (1998) 663.
8 J. P. Dubes, private communication, (1994).
9 J. Lerchner, G. Wolf, A. Torralba and V. Torra, Thermochim. Acta, 302 (1997) 201.
10 J. E. Callanan, J. Thermal Anal., 45 (1995) 359.

11 G. W. H. Höhne and E. Glöggler, Thermochim. Acta, 151 (1989) 295.
12 G. W. H. Höhne, H. K. Cammenga, W. Eysel, E. Gmelin and W. Hemminger, Thermochim. Acta, 160 (1990) 1.
13 I. Wadsö, Thermochim. Acta, 300 (1997) 1.
14 M. J. Richardson, Thermochim. Acta, 300 (1997) 15.
15 G. Currell, 'Instrumentation', John Wiley & Sons (1987) p. 281.
16 V. Torra and H. Tachoire, Thermochim. Acta, 203 (1992) 419.
17 J. L. Macqueron and A. Nouailhat, in 'Microcalorimetry et Thermogenèse', Editions du Centre National de la Recherche Scientifique, Paris, p. 31 (1967).
18 H. Tachoire, J. L. Macqueron and V. Torra, Thermochim. Acta, 105 (1986) 333 (in French).
19 V. Torra and H. Tachoire, J. Thermal Anal., 36 (1990) 1545.
20 G. Guenin, J. L. Macqueron, M. Mantel, C. Auguet, E. Cesari, L. Mañosa, A. Planes, C. Picornell, C. Segui, J. Ortin and V. Torra, Proc. of ICOMAT 86, The Japan Institute of Metals (1987) 794.
21 A. Amengual PhD, (1990) Universitat de les Illes Balears, Palma de Mallorca (Spain) (in Spanish).
22 A. Amengual and V. Torra, J. of Phys. E: Sci. Instrum., 22 (1989) 433.
23 A. Amengual and V. Torra, Thermochim. Acta, 198 (1992) 381.
24 A. Amengual, A. Isalgue, H. Tachoire, V. Torra and V. R. Torra, J. Thermal Anal., 38 (1992) 583.
25 J. Viñals, V. Torra, A. Planes and J. L. Macqueron, Phil. Mag., A 50 (1984) 653.
26 J. Elgueta, J. L. Macqueron and A. Planes, J. Phys.: Condens. Matter., 4 (1992) 285.
27 V. Torra, A. Isalgue and H. Tachoire, Netsu Sokutei, 24 (1997) 179.
28 A. Isalgue and V. Torra, 'Ms-evolution in Cu–Zn–Al SMA. Predictable temperature and time actions on parent phase' ESOMAT'97, Enschede, The Netherlands, J. Phys. IV (1997) C5-339.